

Nuclear suppression of light hadrons and single electrons at RHIC and LHC

B.G. Zakharov

L.D. Landau Institute for Theoretical Physics, GSP-1, 117940,
Kosygina Str. 2, 117334 Moscow, Russia

E-mail: bgz@itp.ac.ru

Abstract. We examine whether it is possible to simultaneously describe the experimental data from RHIC and LHC on nuclear suppression of light hadrons and non-photon single electrons in the pQCD picture of parton energy loss. We perform calculations accounting for both radiative and collisional energy loss. We show that once the coupling constant is fixed from comparison with data on the nuclear modification factor for light hadrons it gives a satisfactory agreement with data on the electron R_{AA} and azimuthal anisotropy v_2 . Our results show that the collisional mechanism is only of marginal significance in nuclear suppression of single electrons except for the bottom contribution at momenta $\lesssim 6 - 8$ GeV.

1. Introduction

A remarkable result of the experiments on AA -collisions at RHIC [1, 2, 3] and LHC [4] is the observation that nuclear suppression of high- p_T single electrons from semi-leptonic decays of heavy mesons is almost as strong as that of pions. It is believed that nuclear suppression of high- p_T particles (jet quenching) is due to radiative [5, 6, 7, 8, 9, 10] and collisional [11] parton energy loss in the hot quark-gluon plasma (QGP) produced in the initial stage of AA -collisions. The observed strong suppression of single electrons indicates that heavy quarks are quenched approximately as light ones. This seemed to be somewhat puzzling in light of the prediction of the dead cone reduction of the heavy quark radiative energy loss [12]. In recent years nuclear suppression of non-photon single electrons due to radiative and collisional heavy quark energy loss in pQCD received considerable theoretical attention [13, 14, 15, 16, 17, 18, 19, 20]. However, no clear consensus has emerged on the physical picture of the effect and whether the pQCD can explain it.

Comparison of the radiative energy loss (calculated within the light-cone path integral (LCPI) approach [7, 21]) and the collisional energy loss calculated with the same α_s and the Debye screening mass shows [22] that for quark energy $E \gtrsim 5$ GeV the collisional energy loss is relatively small for light quarks and c -quark, and for b -quark the collisional energy loss becomes important only at $E \lesssim 10$ GeV. This shows that the collisional energy loss should be of only marginal significance in suppression of single electrons at $p_T \gtrsim 5$ GeV (since the electron spectrum is controlled by heavy quark production at approximately twice the electron momentum). This is also supported from computations of the nuclear modification factor R_{AA} of single electrons for purely collisional mechanism in [19, 20], where it was found that to fit the data the cross sections of the $2 \rightarrow 2$ processes should be enhanced by a factor ~ 4 . Thus, it is natural to expect that, if the pQCD is valid for parton energy loss for RHIC and LHC conditions, the nuclear suppression of single electrons should be described in a picture where the radiative mechanism dominates.

The purpose of the present work is to analyze the available RHIC and LHC data on the electron suppression, and to examine whether the observed nuclear suppression of single electrons and light hadrons can be described simultaneously in the pQCD. In our study we use the LCPI approach [7] to induced gluon emission. The advantage of this formalism is that it treats accurately the mass and finite-size effects, and is valid beyond the soft gluon approximation (used in previous analyses [13, 15, 16, 18]). Calculations beyond the soft gluon approximation are especially desirable for c -quark. Indeed, in the LCPI formalism [7] the induced gluon x -spectrum (x is the gluon fractional momentum) is expressed through the solution of a two-dimensional Schrödinger equation in which the longitudinal coordinate z (along the fast parton momentum) plays the role of time. And the Hamiltonian (see Appendix) depends on the parton masses only through the term $1/L_f = [m_q^2 x^2 + m_g^2 (1-x)^2]/2x(1-x)E$, where E is the initial quark energy, $m_{q,g}$ are the quasiparticle parton masses. The quark mass becomes important when

$m_q^2 x^2 \gtrsim m_g^2 (1-x)^2$. Taking $m_g \sim 400$ MeV [23], we see that it occurs at $x \gtrsim 0.3$ for c -quark and $x \gtrsim 0.1$ for b -quark, and below these values the sensitivity to the quark mass should vanish quickly. Accurate numerical calculations [24] corroborate these qualitative estimates. Note that the results of [24] show that at energy $\sim 10 - 20$ GeV for a finite-size plasma the quark mass suppression of the radiative energy loss may be considerably weaker than predicted in the dead cone model [12], and at higher energies the radiative energy loss may even be enhanced for heavy quarks. Therefore the observed strong suppression of single electrons does not seem to be very strange.

We treat the effect of parton energy loss on the single electron yield within the scheme developed previously for light hadrons [25] (see also [26]). It takes into account both radiative and collisional energy loss, and fluctuations of the fast parton path lengths in the QGP. The calculations of radiative and collisional energy loss are performed with running coupling. In our recent note [27] we analyzed within this approach the flavor dependence of R_{AA} at the LHC energy. In this paper we concentrate on suppression of single electrons and analyze both the RHIC and LHC data. Besides the nuclear modification factor R_{AA} we present results for the azimuthal asymmetry v_2 .

2. Main features of the model

In this section we present the basic features of our approach. We refer the interested reader to Refs. [25, 26] for more details.

We define the nuclear modification factor R_{AA} for a given impact parameter b as

$$R_{AA}(b, \mathbf{p}_T, y) = \frac{dN(A + A \rightarrow h + X)/d\mathbf{p}_T dy}{T_{AA}(b) d\sigma(N + N \rightarrow h + X)/d\mathbf{p}_T dy}, \quad (1)$$

where \mathbf{p}_T is the particle transverse momentum, y is rapidity (we consider the central region around $y = 0$), $T_{AA}(b) = \int d\boldsymbol{\rho} T_A(\boldsymbol{\rho}) T_A(\boldsymbol{\rho} - \mathbf{b})$, T_A is the nucleus profile function. The numerator in (1) is the differential yield of the process $A + A \rightarrow h + X$ (for clarity we omit the argument b) given by

$$\frac{dN(A + A \rightarrow h + X)}{d\mathbf{p}_T dy} = \int d\boldsymbol{\rho} T_A(\boldsymbol{\rho}) T_A(\boldsymbol{\rho} - \mathbf{b}) \frac{d\sigma_m(N + N \rightarrow h + X)}{d\mathbf{p}_T dy}, \quad (2)$$

where $d\sigma_m/d\mathbf{p}_T dy$ is the medium-modified hard cross section. Similarly to the ordinary pQCD formula we write it as

$$\frac{d\sigma_m(N + N \rightarrow h + X)}{d\mathbf{p}_T dy} = \sum_i \int_0^1 \frac{dz}{z^2} D_{h/i}^m(z, Q) \frac{d\sigma(N + N \rightarrow i + X)}{d\mathbf{p}_T^i dy}, \quad (3)$$

where $\mathbf{p}_T^i = \mathbf{p}_T/z$ is the transverse momentum of the initial hard parton, $d\sigma(N + N \rightarrow i + X)/d\mathbf{p}_T^i dy$ is the ordinary hard cross section, $D_{h/i}^m$ is the medium-modified fragmentation function (FF) for transition of a parton i into the observed particle h . For the initial virtuality Q we use the parton momentum p_T^i . As in [25], the hard cross sections on the right-hand side of (3) were calculated using the LO pQCD formula with the CTEQ6 [28] parton distribution functions. The higher order effects were simulated taking for the virtuality scale in α_s the value cQ with $c = 0.265$ as in the

PYTHIA event generator [29]. This prescription gives a fairly good description of the p_T -dependence of the spectra in pp -collisions ‡. We account for the nuclear modification of the parton densities with the EKS98 correction [31] (which gives a small deviation of R_{AA} from unity even without parton energy loss).

The formation length arguments allow, in first approximation, to neglect the overlap between the DGLAP and the induced stages of the parton showering [25]. Then, assuming that formation of the final particle h occurs outside the medium, symbolically the medium-modified FF can be written as

$$D_{h/i}^m(Q) \approx D_{h/j}(Q_0) \otimes D_{j/k}^{in} \otimes D_{k/i}(Q), \quad (4)$$

where \otimes denotes z -convolution, $D_{k/i}$ is the ordinary DGLAP FF for $i \rightarrow k$ parton transition, $D_{j/k}^{in}$ is the FF for $j \rightarrow k$ parton transition in the QGP due to induced gluon emission, and $D_{h/j}$ describes fragmentation of the parton j into the detected particle h outside of the QGP.

We computed the DGLAP FFs using the PYTHIA event generator [29]. For the stage outside the QGP for light partons we use for the $D_{h/j}(Q_0)$ the KKP [32] FFs with $Q_0 = 2$ GeV. We treat the formation of single electrons from heavy quarks as the two-step fragmentations $c \rightarrow D \rightarrow e$ and $b \rightarrow B \rightarrow e$. For the $c \rightarrow D$ and $b \rightarrow B$ transitions we use the Peterson FF with parameters $\epsilon_c = 0.06$ and $\epsilon_b = 0.006$. The z -distribution for the $M \rightarrow e$ transitions (for $M = B/D$) that we need may be expressed via the electron momentum spectrum dB/dp in the heavy meson rest frame as

$$D_{e/M}(z, P) = \frac{P}{4} \int_0^\infty dq^2 \frac{\cosh(\phi - \theta)}{p^2 \cosh \phi} \cdot \frac{dB}{dp}, \quad (5)$$

where $p = \sqrt{(q^2 + m_e^2) \cosh^2(\phi - \theta) - m_e^2}$, $\theta = \text{arcsinh}(P/M)$, $\phi = \text{arcsinh}(zP/\sqrt{q^2 + m_e^2})$, P is the heavy meson momentum, and M is its mass. We evaluated the $B/D \rightarrow e$ FFs using the CLEO data [33, 34] on the electron spectra in the B/D -meson decays. We did not include the $B \rightarrow D \rightarrow e$ process, which gives a negligible contribution [30].

To calculate the FFs $D_{j/k}^{in}$ in the induced stage we use the one gluon spectrum dP/dx computed in the LCPI formalism [7] with the help of the method suggested in [35]. The formulas for calculation of dP/dx are recorded in the Appendix for the reader's convenience. The effect of multiple gluon emission was accounted for using Landau's method as in [36] (see [25] for details). As in [25], for the quasiparticle masses of light quarks and gluon we take $m_q = 300$ and $m_g = 400$ MeV supported by the analysis of the lattice data [23]. The results are practically insensitive to the light quark mass. For heavy quarks we take $m_c = 1.2$ GeV and $m_b = 4.75$ GeV. We use the Debye mass obtained in the lattice calculations [37] giving μ_D/T slowly decreasing with T ($\mu_D/T \approx 3$ at $T \sim 1.5T_c$, $\mu_D/T \approx 2.4$ at $T \sim 4T_c$). We used running α_s frozen at some value α_s^{fr} at low momenta (the technical details for incorporating the running α_s can be found in [35]). For gluon emission in vacuum a reasonable choice is $\alpha_s^{fr} \approx 0.7$ [38, 39].

‡ For the heavy quark cross sections our LO formulas give the p_T -dependences (and the c/b ratio) that agree well with the more sophisticated FONLL calculations [30]. However, the normalization of the cross sections are smaller by a factor $\sim 1/2$. But for R_{AA} it is not important.

However, in the QGP the thermal effects can suppress the α_s^{fr} , and we regard it as a free parameter which should be fixed by the data. If our model is valid, the α_s^{fr} for light hadrons and single electrons should be close to each other.

As in [25], we treat the collisional mechanism as a perturbation to the radiative one. We account for its effect by redefining the initial QGP temperature in calculating the radiative medium-modified FFs according to the condition

$$\Delta E_{rad}(T_0') = \Delta E_{rad}(T_0) + \Delta E_{col}(T_0), \quad (6)$$

where $\Delta E_{rad/col}$ is the radiative/collisional energy loss, T_0 is the real initial temperature of the QGP, and T_0' is the renormalized temperature. We carry out this temperature renormalization for each parton trajectory in the QGP (separately for quarks and gluons). For the collisional energy loss we use the Bjorken method [11] with an accurate treatment of kinematics of the $2 \rightarrow 2$ processes (the details can be found in [22]). For the collisional mechanism we use the same parametrization of $\alpha_s(Q)$ as for the radiative one. Both the radiative and collisional contributions in (6) were calculated for maximum energy transfer constrained by half of the initial parton energy.

3. Numerical results and comparison with the data

We have performed the computations using Bjorken's 1+1D expansion of the QGP [40], which gives $T_0^3 \tau_0 = T^3 \tau$. We take $\tau_0 = 0.5$ fm. In calculating the medium-modified FFs, for simplicity, we neglect variation of the initial temperature T_0 with the transverse coordinates across the overlapping area of two colliding nuclei. We define this area as overlapping of two circles with radius $R = R_A + kd$, where R_A and d are the parameters of the Woods-Saxon nuclear density $\rho_A(r) = \rho_0/[1 + \exp((r - R_A)/d)]$. We take $k = 1.5$, which guarantees that the fraction of the lost QGP volume is negligible. The results are not very sensitive to variation of k in the physically reasonable range $1 \lesssim k \lesssim 2$ (except for very peripheral AA -collisions, which we do not address in the present paper). To fix T_0 (in each centrality bin) we use data on the charged hadron multiplicity pseudorapidity density $dN_{ch}/d\eta$ from RHIC [41] and LHC [42, 43]. For the entropy/multiplicity ratio we use $dS/dy/dN_{ch}/d\eta \approx 7.67$ obtained in [44]. For the chemically equilibrated ideal QGP (we take $N_f = 2.5$) it gives $T_0 \approx 320$ MeV for central Au+Au collisions at $\sqrt{s} = 200$ GeV, and $T_0 \approx 420$ MeV for central Pb+Pb collisions at $\sqrt{s} = 2.76$ TeV. For each hard parton we calculate accurately the path length in the QGP, L , according to the geometry of the AA -collision. Since the QGP should cool quickly at times about 1 – 2 units of the nucleus radius due to transverse expansion [40], we impose the condition $L < L_{max}$. We performed the computations for $L_{max} = 8$. We checked that the bigger value $L_{max} = 10$ fm gives almost the same.

In order to illustrate the relative contribution of the collisional mechanism to parton energy loss in our model, in Fig. 1 we present ΔE_{rad} and ΔE_{col} for light and heavy quarks at $T_0 = 300, 400$ and 500 MeV obtained for $L = 5$ fm, which is a typical parton path length for central AA -collisions at RHIC and LHC. One can see that for light quarks

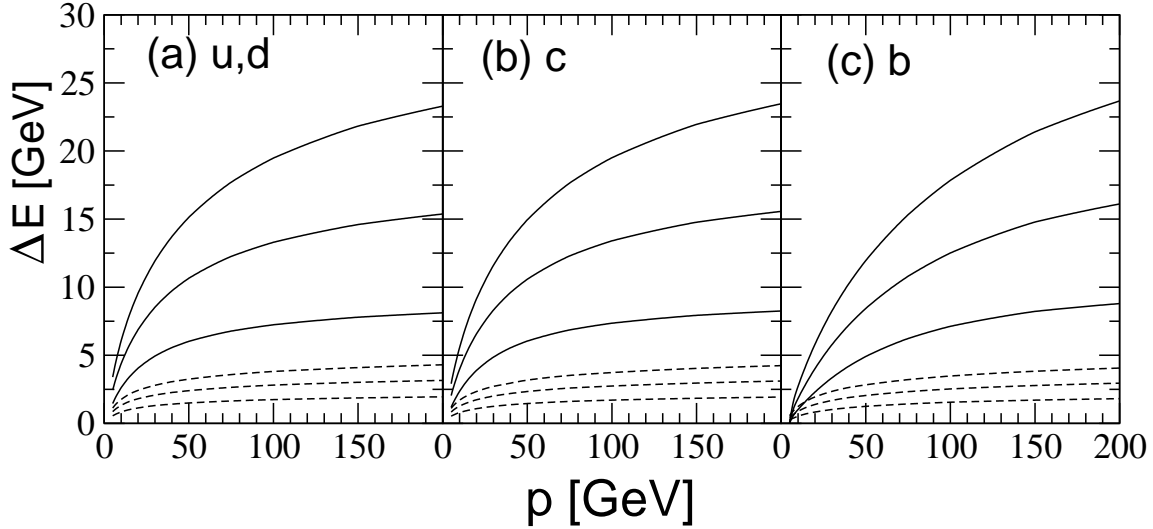


Figure 1. The radiative (solid) and collisional (dashed) energy loss for (a) u, d , (b) c , and (c) b quarks in expanding plasma of size $L = 5$ fm for $T_0 = 300, 400,$ and 500 MeV for $\alpha_s^{fr} = 0.5$. The order of the curves corresponds to ordering of their T_0 .

and c -quarks the contribution of the collisional mechanism is relatively small at $p \gtrsim 5$ GeV. But for b -quarks the collisional mechanism becomes clearly important at $p \lesssim 10$ GeV. In this region our prescription (6) does not apply. From the variation of ΔE for the radiative and collisional mechanisms with the initial plasma temperature in Fig. 1 one can understand the magnitude of the ratio T'_0/T_0 at $T_0 \sim 300 - 400$ MeV relevant to RHIC and LHC. For light quarks and c quark at $p \sim 10 - 50$ GeV $(T'_0/T_0)^3 \sim 1.3 - 1.5$, and for b quark at $p \sim 10 - 20$ GeV this ratio is somewhat larger $\sim 1.5 - 1.8$.

Fig. 2 shows comparison of our predictions for R_{AA} for 0–5% centrality bin for (a) π^0 -meson in Au+Au collisions at $\sqrt{s} = 200$ GeV to PHENIX data [45], and for (b,c) charged hadrons in Pb+Pb collisions at $\sqrt{s} = 2.76$ TeV to (b) ALICE [46] and (c) CMS [47] data. Note that in our calculations based on (4) we ignore possible anomalous baryon contribution [48] to the yield of charged particles. Theoretically it is expected to be small at LHC [48]. In our model with the KKP FFs [32] for the hadronization outside the QGP, R_{AA} for charged hadrons turns out to be very close to that for pions. Experimentally the preliminary data from ALICE [49] on R_{AA} for neutral pions also corroborate this. We present our results for $\alpha_s^{fr} = 0.4$ (upper curves) and 0.5 (lower curves). To illustrate the effect of collisional energy loss we show the total R_{AA} with radiative and collisional energy loss (solid) and for purely radiative energy loss (dashed). One can see that the effect of the collisional mechanism is relatively small (especially for LHC). We present the results for $p_T \gtrsim 5$ GeV since for smaller momenta our calculations of the induced gluon emission (based on the relativistic approximation) are hardly robust. Fig. 2 shows that for light hadrons the window $\alpha_s^{fr} \sim 0.4 - 0.5$ leads to a reasonable magnitude of R_{AA} . However, the agreement in the shape of the p_T -dependence of R_{AA} is evidently not perfect. But this discrepancy does not seem

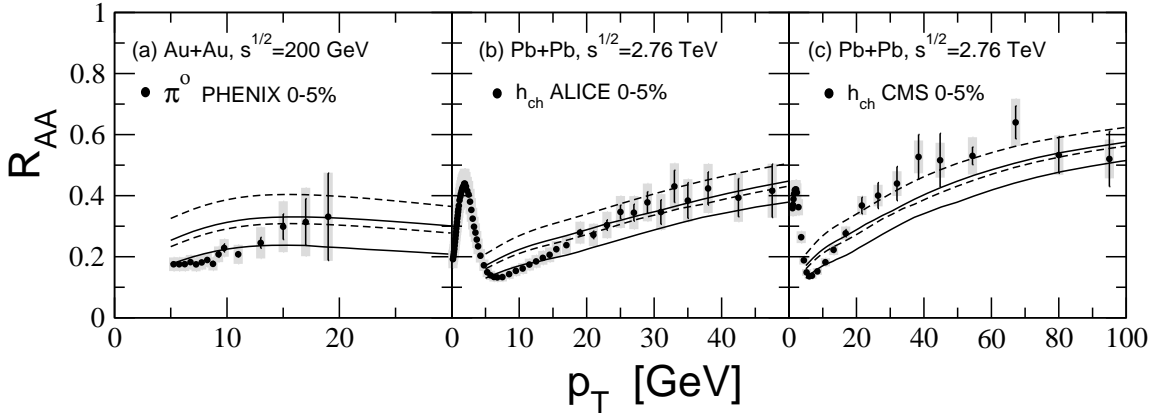


Figure 2. (a) R_{AA} for π^0 for 0-5% central Au+Au collisions at $\sqrt{s} = 200$ GeV from our calculations compared to data from PHENIX [45]. (b,c) R_{AA} for charged hadrons for 0-5% central Pb+Pb collisions at $\sqrt{s} = 2.76$ GeV from our calculations compared to data from (b) ALICE [46] and (c) CMS [47]. Systematic experimental errors are shown as shaded areas. The curves show our calculations for radiative and collisional energy loss (solid), and for purely radiative energy loss (dashed) for $\alpha_s^{fr} = 0.4$ (upper curves) and 0.5 (lower curves).

to be very dramatic since the theoretical uncertainties of the approximations involved may be significant. One of the most serious sources of the theoretical errors, that can be important for the p_T -dependence of R_{AA} , is the Landau approximation for multiple gluon emission [36]. As can be seen from Fig. 2a for RHIC the agreement of the theoretical R_{AA} (radiative plus collisional energy loss) with the data is better for $\alpha_s^{fr} = 0.5$. Figs. 2b,c show that for LHC the value $\alpha_s^{fr} = 0.4$ seems to be preferred by the data (if one considers the complete p_T range). Thus, the values $\alpha_s^{fr} = 0.5$ and 0.4 seem to be reasonable benchmarks for calculations of the nuclear modification factor of single electrons at RHIC and LHC energies. The tendency of the decrease of α_s^{fr} from RHIC to LHC, first observed in [26], is natural, since the thermal reduction of α_s should be stronger at the LHC energies. In fact, the variation of α_s^{fr} may be stronger if one takes $\tau_0^{RHIC} > \tau_0^{LHC}$, which seems to be quite reasonable since from the dimension arguments one can expect $\tau_0 \propto 1/T_0$. However, our purpose is to study the variation of nuclear suppression from light flavors to heavy ones probed via single electrons, and for this reason it is sufficient to have just α_s^{fr} fixed at each energy from the light hadron data.

In Fig. 3 we compare results of our model with STAR [2] and PHENIX [3] data on the electron R_{AA} . Comparison to the data from ALICE [4] is shown in Fig. 4a. In Fig. 3, 4a we show the total (charm plus bottom) R_{AA} with (solid) and without (dashed) collisional energy loss. From Figs. 3, 4a one sees that our pQCD model for the same window of α_s^{fr} as for light hadrons leads to quite satisfactory agreement with data on the electron R_{AA} . Similarly to R_{AA} for light hadrons the electron data support $\alpha_s^{fr} \approx 0.5$ for RHIC, and $\alpha_s^{fr} \approx 0.4$ for LHC. Thus, the simultaneous description of the

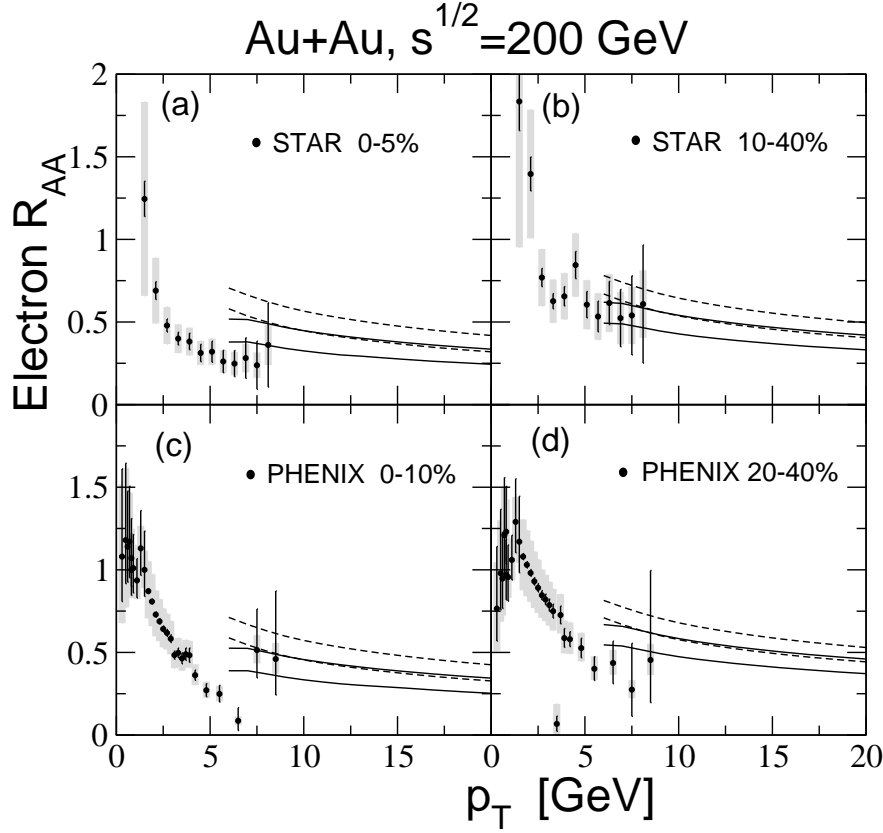


Figure 3. The electron R_{AA} in Au+Au collisions at $\sqrt{s} = 200$ GeV for (a) 0–5%, (b) 10–40%, (c) 0–10%, (d) 20–40% centrality classes. The curves show calculations for radiative and collisional energy loss (solid), and for purely radiative energy loss (dashed) including charm and bottom contributions for $\alpha_s^{fr} = 0.4$ (upper curves) and 0.5 (lower curves). Data points are from STAR [2] and PHENIX [3]. Systematic errors are shown as shaded areas.

nuclear suppression of light hadrons and single electrons in the pQCD picture seems quite possible. Of course, this should be taken with a caution since the overlapping of the p_T region, where our approximations make sense, with that studied experimentally is still rather narrow (especially for RHIC), and namely in this region the experimental errors are very large.

To illustrate the effect of collisional energy loss for $c \rightarrow e$ and $b \rightarrow e$ processes in Fig. 4b we show the curves for R_{AA} separately for charm (thick) and bottom (thin) with (solid) and without (dashed) collisional energy loss for $\alpha_s^{fr} = 0.4$. One sees that the collisional mechanism is more important for bottom. The effect becomes especially significant at low p_T . At $p_T \lesssim 5-6$ GeV our treatment of the collisional mechanism as a perturbation to the radiative one, with the help of (6), loses accuracy. Evidently, in this regime the radiative and collisional mechanisms must be treated on an equal footing. However, a solution of this challenging problem is still lacking. For charm the situation is better, since across the whole energy range, where the relativistic approximation makes sense, the collisional energy loss remains relatively small. Note that, as one can see from

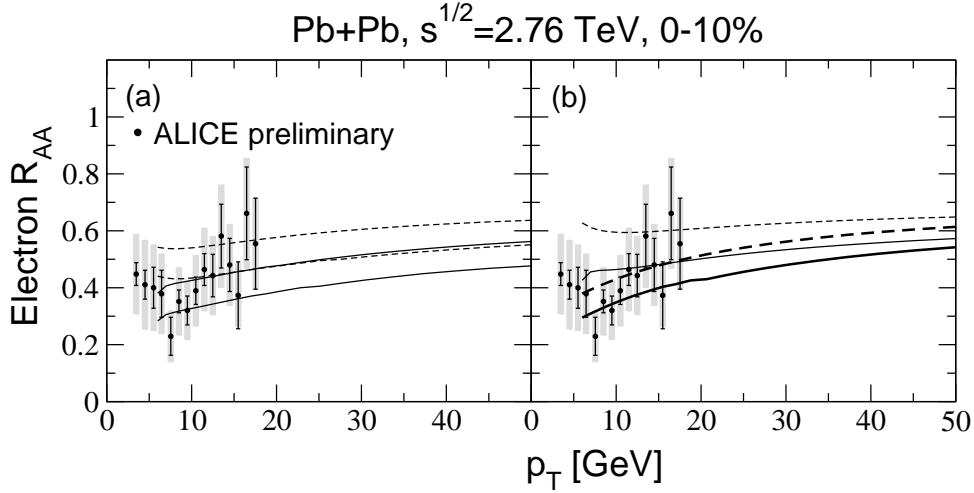


Figure 4. (a) The electron R_{AA} for 0-10% central Pb+Pb collisions at $\sqrt{s} = 2.76$ TeV for $\alpha_s^{fr} = 0.4$ (upper curves) and 0.5 (lower curves) including charm and bottom. The experiment points are the preliminary ALICE data [4]. Systematic errors are shown as shaded areas. (b) The electron R_{AA} for charm (thick) and bottom (thin) contributions at $\alpha_s^{fr} = 0.4$. In (a,b) the solid curves show results for radiative plus collisional energy loss, and the dashed curves for purely radiative energy loss.

Fig. 4b, the difference between the charm and bottom suppression factors at $p_T \gtrsim 6$ GeV is relatively small. For this reason the total (charm plus bottom) R_{AA} is quite stable against variation of the b/c ratio which is not very robust. Even at $p_T \sim 6 - 10$ GeV variation in b/c ratio of $\pm 30\%$ changes the total R_{AA} by $\pm(2 \div 3)\%$.

It is interesting to compare with the data the theoretical predictions for the electron azimuthal anisotropy v_2 , which is sensitive to the L -dependence of the heavy quark energy loss. In Fig. 5 we compare our calculations for the 20–40% centrality bin to v_2 from (a) PHENIX [3] and (b) ALICE [4]. One sees that the agreement with the ALICE data is fairly good. However, the experimental errors are very large and the p_T range is too limited to make a definitive conclusion on the preferred value of α_s^{fr} . For the PHENIX data [3] $p_T \lesssim 4$ GeV. For such low p_T our calculations are not robust. Nevertheless, our v_2 for $\alpha_s^{fr} = 0.5$ (favored by data on R_{AA} for pions) at $p_T = 6$ GeV matches reasonably well the experimental v_2 at $p_T \approx 4$ GeV.

Note that our predictions were obtained with the radiative energy loss for the QGP modelled by a system of the static Debye screened color centers [5]. The generalization to the dynamical QGP described within the HTL scheme is trivial (see [50] for details). It is reduced to replacement of the potential (A4) (let us call it v_{stat}) by a dynamical potential v_{dyn} , which can be expressed through the gluon polarization operator. In the HTL scheme an elegant formula derived in [51] allows to write v_{dyn} similarly to the static case just replacing the factor $1/(q^2 + \mu_D)^2$ by $1/[q^2(q^2 + \mu_D)]$ in the formula for the dipole cross section (A6), and increasing a little the overall normalization by a factor $\frac{\pi^2}{6 \cdot 1.202}(1 + N_f/6)/(1 + N_f/4) \approx 1.19$ (for $N_f = 2.5$). This modification leads to unlimited growth of v_{dyn} at large ρ (due to zero magnetic mass in the HTL approximation), while

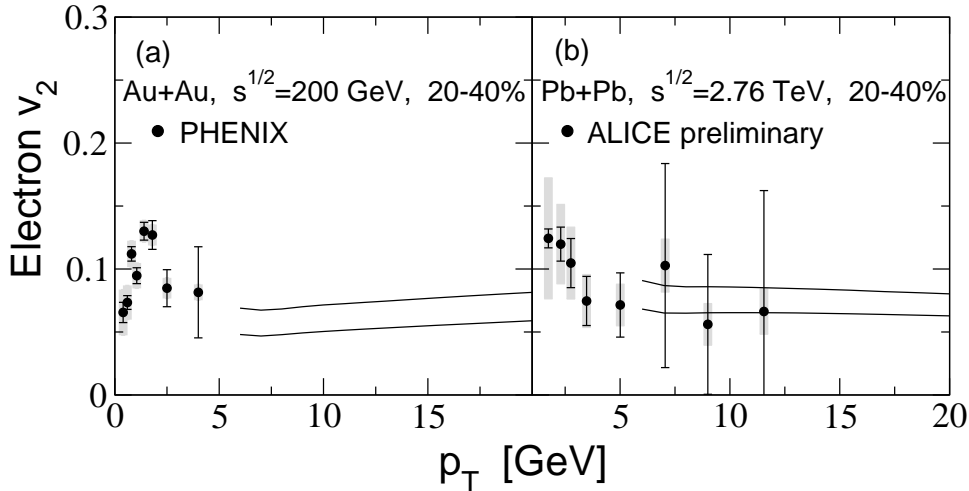


Figure 5. v_2 for single electrons for 20–40% centrality class in (a) Au+Au collisions at $\sqrt{s} = 200$ GeV, and in (b) Pb+Pb collisions at $\sqrt{s} = 2.76$ TeV. The theoretical curves are for $\alpha_s^{fr} = 0.4$ (lower curves), and 0.5 (upper curves), and include both the charm and bottom contributions. Data points are from (a) PHENIX [3], and (b) ALICE [4]. Systematic errors are shown as shaded areas.

v_{stat} flattens at $\rho \gtrsim 1/m_D$. It has been recently claimed [18] that the dynamical effects enhance the heavy flavor suppression, and are important for description of the single electron suppression. Of course, modification of the potential in the above manner for the dynamical QGP should enhance the heavy quark suppression. However, this enhancement itself is uninteresting in the context of the heavy-to-light ratio $R_{AA}^{heavy}/R_{AA}^{light}$ since the dynamical potential should enhance the light flavor suppression as well. One can expect that the dynamical effects affect the induced gluon emission for light and heavy flavors similarly. Indeed, the dominating ρ -region for induced gluon emission for light and heavy flavors[§], is $\rho \lesssim \sqrt{S_{LPM}}/m_g$ [7] (here S_{LPM} is the suppression factor due to the Landau-Pomeranchuk-Migdal effect, which is typically not very small ($\sim 0.2 - 0.5$) for RHIC and LHC). In this ρ -region the shapes of $v_{dyn}(\rho)$ and $v_{stat}(\rho)$ are qualitatively very similar. For this reason modification of the nuclear suppression due to the dynamical effects should be similar for light and heavy flavors. And, once the coupling is fixed by the data on R_{AA} for light hadrons, the dynamical formulation should give R_{AA} for heavy flavors (and single electrons) close to that for the static model. We have checked this performing numerical calculations (for a fixed coupling constant as in the HTL scheme), and have found a negligible modification of the heavy-to-light ratio for the dynamical model. Note that the use of the $v_{dyn}(\rho)$ hardly makes the calculations more robust. Indeed, the difference between $v_{dyn}(\rho)$ and $v_{stat}(\rho)$ at $\rho \gtrsim 1/m_D$ is related mostly to the zero magnetic mass in the HTL scheme. But the lattice calculations [53] show that in reality the magnetic mass may be of the order of the electric Debye mass.

[§] For heavy quarks the typical ρ becomes smaller than for light partons only in the tail region $x \gtrsim m_g/m_Q$, where quark mass suppresses strongly gluon emission.

On the other hand, in the region $\rho \ll 1/m_D$, where the HTL approximation is not supposed to be valid, it gives incorrect normalization of the potential (contrary to the static model, which gives the correct result at $\rho \rightarrow 0$).

4. Summary

In this paper we have examined whether it is possible in the pQCD picture of the parton energy loss to simultaneously describe experimental data from RHIC and LHC on nuclear suppression of light hadrons and single electrons from the heavy meson decays. We have performed calculations taking into account radiative and collisional energy loss, and fluctuations of the fast parton path lengths in the QGP. The calculations of radiative energy loss have been performed within the LCPI approach [7]. Both radiative and collisional energy loss were computed with running α_s frozen at low momenta at some value α_s^{fr} .

We have found that once the value of α_s^{fr} is fixed from the data on the nuclear modification factor for light hadrons it gives a satisfactory agreement with the data on the electron R_{AA} as well. For the electron azimuthal anisotropy v_2 the agreement is also within the experimental errors. Our calculations show that the effect of collisional energy loss is relatively small, and cannot be crucial for the flavor dependence of the nuclear suppression factor for $p_T \gtrsim 10$ GeV. The collisional mechanism becomes very important only for the bottom contribution to the electron spectrum at momenta $\lesssim 6-8$ GeV.

Our results, together with fairly good agreement with the ALICE LHC data on R_{AA} of D -mesons [54, 55] obtained in our recent analysis [27], give support for the pQCD picture of parton energy loss both for light and heavy flavors. However, the available data on the nuclear suppression of single electrons, especially from RHIC, analyzed in the present work, are restricted to rather low p_T , where the conditions of applicability of our pQCD model may be not good enough. For more conclusive test of the model it is highly desirable to have data on the electron R_{AA} that extend to larger values of p_T .

Note that measurement of the electron R_{AA} at larger p_T (say, for $p_T \sim 50$ GeV that corresponds to heavy quark momenta ~ 100 GeV) at LHC is especially desirable in the light of the preliminary CMS data [56] on the b -jet R_{AA} in Pb+Pb collisions at $\sqrt{s} = 2.76$ TeV, which has been measured to be $0.48 \pm 0.09(\text{stat.}) \pm 0.18(\text{syst.})$ at $100 < p_T < 120$ GeV for 0–100% centrality, while for inclusive jets $R_{AA} = 0.5 \pm 0.01(\text{stat.}) \pm 0.06(\text{syst.})$. This result, if confirmed by future more accurate measurements, will be a serious challenge for the pQCD picture of jet quenching. Indeed, from Fig. 1 one can see that at $p_T \gtrsim 100$ GeV the energy losses for light quarks and b -quarks become very close, and their jet R_{AA} should be close as well. But at $p_T \sim 100 - 120$ GeV $\sim 60 - 70\%$ of inclusive jets are gluon jets that have energy loss enhanced by a factor $\sim 9/4$, and should have R_{AA} smaller than that for light and heavy quarks. For this reason the inclusive jet R_{AA} should be smaller than that for b -jets.

Acknowledgements

I am indebted to the referee, who remarked on the preliminary CMS data [56] on the b -jet R_{AA} . This work is supported in part by the grant RFBR 12-02-00063-a and the program SS-6501.2010.2.

Appendix: Formulas for one gluon x -spectrum

We use the representation of the one gluon emission x -distribution obtained in [35] which is convenient for numerical calculations. For $q \rightarrow gq$ process it reads

$$\frac{dP}{dx} = \int_0^L dz n(z) \frac{d\sigma_{eff}^{BH}(x, z)}{dx}, \quad (\text{A1})$$

where $n(z)$ is the medium number density, $d\sigma_{eff}^{BH}/dx$ is an effective Bethe-Heitler cross section accounting for both the Landau-Pomeranchuk-Migdal and finite-size effects. The $d\sigma_{eff}^{BH}/dx$ reads

$$\frac{d\sigma_{eff}^{BH}(x, z)}{dx} = -\frac{P_q^g(x)}{\pi M} \text{Im} \int_0^z d\xi \alpha_s(Q^2(\xi)) \frac{\partial}{\partial \rho} \left(\frac{F(\xi, \rho)}{\sqrt{\rho}} \right) \Big|_{\rho=0}. \quad (\text{A2})$$

Here $P_q^g(x) = C_F[1 + (1-x)^2]/x$ is the usual splitting function for $q \rightarrow gq$ process, $M = Ex(1-x)$ is the reduced "Schrödinger mass", $Q^2(\xi) = aM/\xi$ with $a \approx 1.85$ [22], F is the solution to the radial Schrödinger equation for the azimuthal quantum number $m = 1$

$$i \frac{\partial F(\xi, \rho)}{\partial \xi} = \left[-\frac{1}{2M} \left(\frac{\partial}{\partial \rho} \right)^2 + v(\rho, x, z - \xi) + \frac{4m^2 - 1}{8M\rho^2} + \frac{1}{L_f} \right] F(\xi, \rho) \quad (\text{A3})$$

with the boundary condition $F(\xi = 0, \rho) = \sqrt{\rho} \sigma_3(\rho, x, z) \epsilon K_1(\epsilon \rho)$ (K_1 is the Bessel function), $L_f = 2M/\epsilon^2$ with $\epsilon^2 = m_q^2 x^2 + m_g^2 (1-x)^2$, $\sigma_3(\rho, x, z)$ is the cross section of interaction of the $q\bar{q}g$ system with a medium constituent located at z . The potential v in (A3) reads

$$v(\rho, x, z) = -i \frac{n(z) \sigma_3(\rho, x, z)}{2}. \quad (\text{A4})$$

The σ_3 is given by [52]

$$\sigma_3(\rho, x, z) = \frac{9}{8} [\sigma_{q\bar{q}}(\rho, z) + \sigma_{q\bar{q}}((1-x)\rho, z)] - \frac{1}{8} \sigma_{q\bar{q}}(x\rho, z), \quad (\text{A5})$$

where

$$\sigma_{q\bar{q}}(\rho, z) = C_T C_F \int d\mathbf{q} \alpha_s^2(q^2) \frac{[1 - \exp(i\mathbf{q}\boldsymbol{\rho})]}{[q^2 + \mu_D^2(z)]^2} \quad (\text{A6})$$

is the local dipole cross section for the color singlet $q\bar{q}$ pair ($C_{F,T}$ are the color Casimir for the quark and thermal parton (quark or gluon), μ_D is the local Debye mass).

For $g \rightarrow gg$ one should replace the splitting function and m_q by m_g in ϵ^2 . The σ_3 in this case reads

$$\sigma_3(\rho, x, z) = \frac{9}{8} [\sigma_{q\bar{q}}(\rho, z) + \sigma_{q\bar{q}}((1-x)\rho, z) + \sigma_{q\bar{q}}(x\rho, z)]. \quad (\text{A7})$$

References

- [1] S.S. Adler *et al.* [PHENIX Collaboration], Phys. Rev. Lett. **96**, 032301 (2006).
- [2] B.I. Abelev *et al.* [STAR Collaboration], Phys. Rev. Lett. **98**, 192301 (2007) [arXiv:nucl-ex/0607012], Erratum-ibid. 106 (2011) 159902.
- [3] A. Adare *et al.* [PHENIX Collaboration], Phys. Rev. **C84**, 044905 (2011).
- [4] S. Sakai, for the ALICE Collaboration, contribution to the Quark Matter 2012 Conf., <http://qm2012.bnl.gov/default.asp>.
- [5] M. Gyulassy and X.N. Wang, Nucl. Phys. **B420**, 583 (1994).
- [6] R. Baier, Y.L. Dokshitzer, A.H. Mueller, S. Peigné, and D. Schiff, Nucl. Phys. **B483**, 291 (1997); *ibid.* **B484**, 265 (1997); R. Baier, Y.L. Dokshitzer, A.H. Mueller, and D. Schiff, Nucl. Phys. **B531**, 403 (1998).
- [7] B.G. Zakharov, JETP Lett. **63**, 952 (1996); *ibid* **65**, 615 (1997); **70**, 176 (1999); Phys. Atom. Nucl. **61**, 838 (1998).
- [8] U.A. Wiedemann, Nucl. Phys. **A690**, 731 (2001).
- [9] M. Gyulassy, P. Lévai, and I. Vitev, Nucl. Phys. **B594**, 371 (2001).
- [10] P. Arnold, G.D. Moore, and L.G. Yaffe, JHEP **0206**, 030 (2002).
- [11] J.D. Bjorken, Fermilab preprint 82/59-THY (1982, unpublished).
- [12] Y.L. Dokshitzer and D.E. Kharzeev, Phys. Lett. **B519**, 199 (2001).
- [13] N. Armesto, M. Cacciari, A. Dainese, C.A. Salgado and U.A. Wiedemann, Phys. Lett. **B637**, 362 (2006).
- [14] M. Djordjevic, J. Phys. **G32**, S333 (2006) [arXiv:nucl-th/0610054].
- [15] S. Wicks, W. Horowitz, M. Djordjevic and M. Gyulassy, Nucl. Phys. **A783**, 493 (2007).
- [16] S. Wicks and M. Gyulassy, J. Phys. **G34**, S989 (2007) [arXiv:nucl-th/0701088].
- [17] P.B. Gossiaux, J. Aichelin, T. Gousset, and V. Guinho, J. Phys. **G37**, 094019 (2010).
- [18] M. Djordjevic, Phys. Rev. **C85**, 034904 (2012).
- [19] A. Meistrenko, A. Peshier, J. Uphoff, and C. Greiner, Nucl. Phys. **A901**, 51 (2013).
- [20] J. Uphoff, O. Fochler, Z. Xu and C. Greiner, arXiv:1208.1970.
- [21] R. Baier, D. Schiff, and B.G. Zakharov, Ann. Rev. Nucl. Part. **50**, 37 (2000) [arXiv:hep-ph/0002198].
- [22] B.G. Zakharov, JETP Lett. **86**, 444 (2007) [arXiv:0708.0816].
- [23] P. Lévai and U. Heinz, Phys. Rev. **C57**, 1879 (1998).
- [24] P. Aurenche and B.G. Zakharov, JETP Lett. **90**, 237 (2009) [arXiv:0907.1918].
- [25] B.G. Zakharov, JETP Lett. **88**, 781 (2008) [arXiv:0811.0445].
- [26] B.G. Zakharov, JETP Lett. **93**, 683 (2011) [arXiv:1105.2028].
- [27] B.G. Zakharov, JETP Lett. **96**, 616 (2013) [arXiv:1210.4148].
- [28] S. Kretzer, H.L. Lai, F. Olness, and W.K. Tung, Phys. Rev. **D69**, 114005 (2004).
- [29] T. Sjostrand, L. Lonnblad, S. Mrenna, and P. Skands, arXiv:hep-ph/0308153.
- [30] M. Cacciari, P. Nason, and R. Vogt, Phys. Rev. Lett. **95**, 122001 (2005).
- [31] K.J. Eskola, V.J. Kolhinen, and C.A. Salgado, Eur. Phys. J. **C9**, 61 (1999).
- [32] B.A. Kniehl, G. Kramer, and B. Potter, Nucl. Phys. **B582**, 514 (2000).
- [33] A.H. Mahmood *et al.* [CLEO Collaboration], Phys. Rev. **D70**, 032003 (2004).
- [34] R. Poling, invited talk at 4th Flavor Physics and CP Violation Conference, Vancouver, British Columbia, Canada, 9-12 Apr 2006, arXiv:hep-ex/0606016.
- [35] B.G. Zakharov, JETP Lett. **80**, 617 (2004) [arXiv:hep-ph/0410321].
- [36] R. Baier, Yu.L. Dokshitzer, A.H. Mueller, and D. Schiff, JHEP **0109**, 033 (2001).
- [37] O. Kaczmarek and F. Zantow, Phys. Rev. **D71**, 114510 (2005).
- [38] N.N. Nikolaev and B.G. Zakharov, Phys. Lett. **B327**, 149 (1994).
- [39] Yu.L. Dokshitzer, V.A. Khoze, and S.I. Troyan, Phys. Rev. **D53**, 89 (1996).
- [40] J.D. Bjorken, Phys. Rev. **D27**, 140 (1983).
- [41] B.I. Abelev *et al.* [STAR Collaboration], Phys. Rev. **C79**, 034909 (2009).

- [42] S. Chatrchyan *et al.* [CMS Collaboration], JHEP **1108**, 141 (2011).
- [43] K. Aamodt *et al.* [ALICE Collaboration], Phys. Rev. Lett. **106**, 032301 (2011).
- [44] B. Müller and K. Rajagopal, Eur. Phys. J. **C43**, 15 (2005).
- [45] A. Adare *et al.* [PHENIX Collaboration], arXiv:1208.2254.
- [46] B. Abelev *et al.* [ALICE Collaboration], Phys. Lett. **B720**, 52 (2013).
- [47] S. Chatrchyan *et al.* [CMS Collaboration], Eur. Phys. J. **C72**, 1945 (2012).
- [48] P. Aurenche and B.G. Zakharov, Eur. Phys.J. **C71**, 1829 (2011) [arXiv:1109.6819].
- [49] D. Peressounko, for the ALICE Collaboration, contribution to the Quark Matter 2012 Conf., <http://qm2012.bnl.gov/default.asp>.
- [50] P. Aurenche and B.G. Zakharov, JETP Lett. **85**, 149 (2007).
- [51] P. Aurenche, F. Gelis and H. Zaraket, JHEP **0205**, 043 (2002).
- [52] N.N. Nikolaev and B.G. Zakharov, Z. Phys. **C64**, 631 (1994).
- [53] A. Cucchieri, F. Karsch, and P. Petreczky, Phys. Lett. **B497**, 80 (2001).
- [54] B. Abelev *et al.* [ALICE Collaboration], JHEP **1209**, 112 (2012) [arXiv:1203.2160].
- [55] A. Grelli, for the ALICE Collaboration, contribution to the Quark Matter 2012 Conf., <http://qm2012.bnl.gov/default.asp>
- [56] CMS Collaboration, CMS Physics Analysis Summary CMS-HIN-12-003, CMS, (2012).